Acta Spartae Vol. 6 No. 1 2022
Pages 11–14

Examining the First Ultra-Compact Dwarf with a Resolved Extended Halo

Allison Jones and Denija Crnojevic[1]

Department of Chemistry, Biochemistry, and Physics, University of Tampa, Tampa, FL 33606, [1]Faculty Advisor

ABSTRACT

Ultra-compact dwarf galaxies are a class of compact galaxies and are among the densest stellar systems in the Universe (Seth et al. , 2014). Since these ultra-compact dwarfs (UCDs) have only been discovered in the last two decades, their formation is still unknown Pfeffer et al. (2014). One hypothesis for their formation, the motive behind this research, is that UCD originate as Nuclear Star Clusters (NSCs) in the central regions of low-mass galaxies, and they develop into these ultra-compact objects after gravitational interaction with a more massive galaxy (Evstigneeva et al. , 2007). In order to investigate whether or not this hypothesis is true, the first step is to determine if these UCDs have any characteristics of a NSC. The UCD that we focused on throughout this research is CenA-MM-UCD1, which lies in the halo of its host galaxy Centaurus A. CenA-MM-UCD1 was selected for further study because it is the first ultra-compact dwarf that has a resolved extended halo. This is a sign that this galaxy could be in a state of disruption from its host galaxy and, based on our hypothesis, could be transitioning from a NSC to a UCD. Throughout this study of CenA-MM-UCD1, we use images from the Hubble Space Telescope to determine if our hypothesis is true.

1 INTRODUCTION

The Panoramic Imaging Survey of Centaurus and Sculptor (PISCeS) was performed with a telescope in Chile to study the closest massive elliptical galaxy, Centaurus A (Crnojević et al., 2016). Within this survey, CenA-MM-UCD1, our target galaxy, was discovered in the outer regions of Centaurus A. This UCD, located 3.7 Mpc from us, is peculiar because of its resolved extended halo, which is unlike ”normal” UCDs. The latter are compact in the center and contain almost no stars in their outskirts. However, CenA-MM-UCD1 is not only densely populated in its central regions, but also displays a diffuse stellar component in its outskirts (see Fig. 1). Further imaging was requested using the Wide Field Camera 3 (WFC3) aboard the Hubble Space Telescope.

The origin of UCDs is still unknown, but evidence suggests they are formed from tidally stripped nuclei of low-mass galaxies (e.g. Evstigneeva et al. , 2007; Pfeffer et al. , 2014; Seth et al. , 2014). CenA-MM-UCD1 may represent a connection between a nuclear star cluster (pre-stripping phase) and a ”normal” UCD (post-stripping phase). In order to determine if this UCD is in transition from a NSC to an UCD, we need to determine if CenA-MM-UCD1 has any characteristics of a NSC. The characteristics of NSCs that are deemed significant are a younger population of stars, a metallicity gradient, and signs of asymmetry or elongation due to the interaction with the host galaxy (Centaurus A).

NSCs contain a spread in age and metallicity (Seth et al. , 2010). To analyze the ages of CenA-MM-UCD's population of stars, we need to create a color-magnitude diagram (CMD) using the images from the Hubble Space Telescope. A CMD is a plot of brightness vs. surface temperature of a star and the star's position on a CMD tells us about the age and metallicity of the star (Crnojević et al., 2016). We use the CMD to determine the age of the stars within our galaxy. To determine the metallicities of the stars, we plot isochrones on our color-magnitude diagram. Isochrones are stellar evolutionary models at a fixed age and they represent how a star will evolve based on a certain metallicity. We match specific models to our CMD and determine the average metallicity of our UCD. In order to determine if CenA-MM-UCD1 is in a state of disruption, we create and analyze a density map of the stars within our galaxy to look for any signs of asymmetry or elongation.

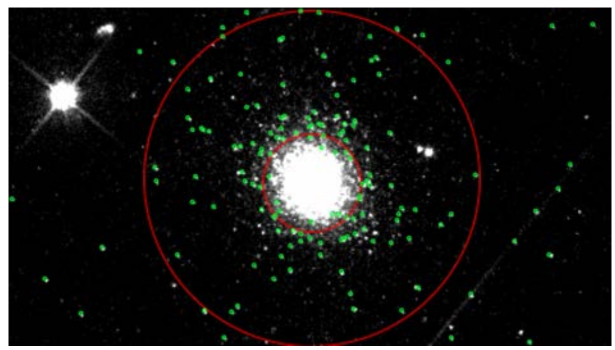

Fig. 1. Image from the Hubble Space Telescope where the inner circle contains the inner portion of the galaxy (a distance of 65 pixels, about 3.25 kpc, or less from the center) and the outer circle contains the outer portion of the galaxy (a distance between 65 and 200, about 10 kpc, pixels from the center), indicating the extended halo. The stars circled in green are the red-giant branch stars that remained after applying our quality cuts. The center of the galaxy does not contain any green stars because they are too close to be individually resolved by the telescope. The large star to the left of our target is a foreground star belonging to the Milky Way.

2 METHODS

Photometry and Data Analysis

To analyze the images of CenA-MM-UCD1 from the Hubble Space Telescope, we perform photometry with a semi-automated program, DOLPHOT[1]. Photometry is the measurement of light released by an astrophysical source, which is observed with different filters and wavelengths. After performing the photometry, we need to eliminate the ”bad” point source detections from our data using quality cuts. These ”bad” stars could be foreground stars from the Milky Way

[1] (http://americano.dolphinsim.com/dolphot/)

Licensed under CC0

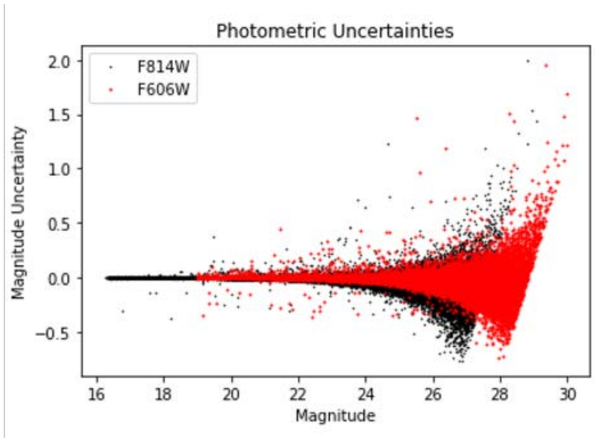

Fig. 2. This plot represents the uncertainty in magnitude as a function of increasing magnitude (larger magnitudes correspond to dimmer objects). As the magnitude increases, the uncertainty also increases because as the stars become dimmer, it is harder to resolve them. The uncertainty was determined from the artificial star tests as the difference between the real and the recovered magnitude values. The black points represent the F814W filter and the red points represent the F606W filter.

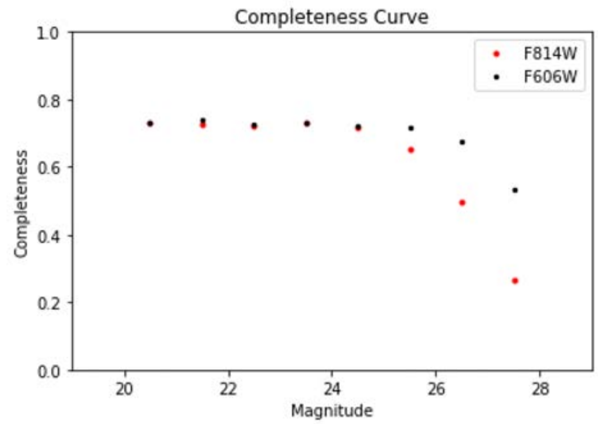

Fig. 3. This curve represents the amount of stars recovered by our photometry out of the total number of injected artificial stars. As the magnitude increases, the amount of stars recovered decreases causing the overall completeness to decrease as well.

galaxy or galaxies so distant that they appear as point sources or stars. The quality cuts allow us to eliminate any stars that could contaminate our data. The quality cuts that we use are object type, error flag, crowding, sharpness, and magnitude error. The limit for the object type is ≤ 2, which eliminated objects from our data that were too extended or too sharp. The error flag is set equal to zero, which eliminated objects that are too saturated or photometry that extend out of the chip. The sharpness parameter is set to be no larger than 0.075. The crowding parameter is set to be smaller than 1, measured in magnitude, quantifying how much brighter the star would be if it was isolated when measured. Lastly, the magnitude error parameter is set to be no greater than 0.3. With these quality cuts, we are able to analyze only the best of our data.

The next step was to determine the uncertainty of the photometry. In order to do this, we perform artificial star tests. This consists of injecting fake stars of known position and magnitude into the image and performing photometry again to recover their properties, using the same quality cuts as before. This allows us to find the uncertainties and completeness for our target (see Fig 2 and 3). The magnitude uncertainty on the y-axis is the difference between the real and recovered magnitudes values. In Fig 2, the uncertainty in magnitude becomes larger, with increasing magnitude. The larger magnitudes correspond to fainter brightness. As the star becomes dimmer, the photometry becomes less accurate and, therefore, more uncertain. Our images were taken using two different filters, F814W and F606W, which represent two different wavelengths in the visible range. The red dots in Fig 2 represent the stars from the F606W filter and the black dots represent the stars from the F814W filter. Fig. 3 shows the amount of stars recovered by our photometry out of the total number of injected artificial stars. A completeness of 1 corresponds to 100 % detection. As the magnitude increases, the amount of stars recovered decreases. From Fig 2 and 3, we are able determine the range in magnitude that produces the best results for our research, which is magnitude values < 25.2 for the F606W filter and < 24 for the F814W filter.

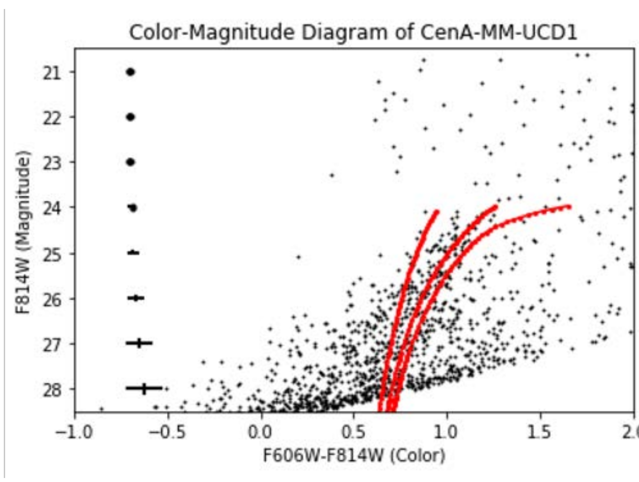

Fig. 4. A color-magnitude diagram of CenA-MM-UCD1 with stellar evolutionary models of differing metal content in red. On the left side, the color and magnitude error bars are shown (as derived in Fig 2). Metallicity is determined by a star's [Fe/H] value, which is a logarithmic quantity based on the Sun. Stars with a positive [Fe/H] value are more metal-rich than the Sun and stars with a negative [Fe/H] value are more metal-poor. The models located towards the right of the plot represent the metal-rich stars and the models located towards the left represent the metal-poor stars. The left-most model has a [Fe/H] value of -2.5, the center model is -1.0, and the right-most model is -0.7, but all three are fixed at an age of 10 Gyrs. The average metallicity value of the stars within the RGB is about -1.4.

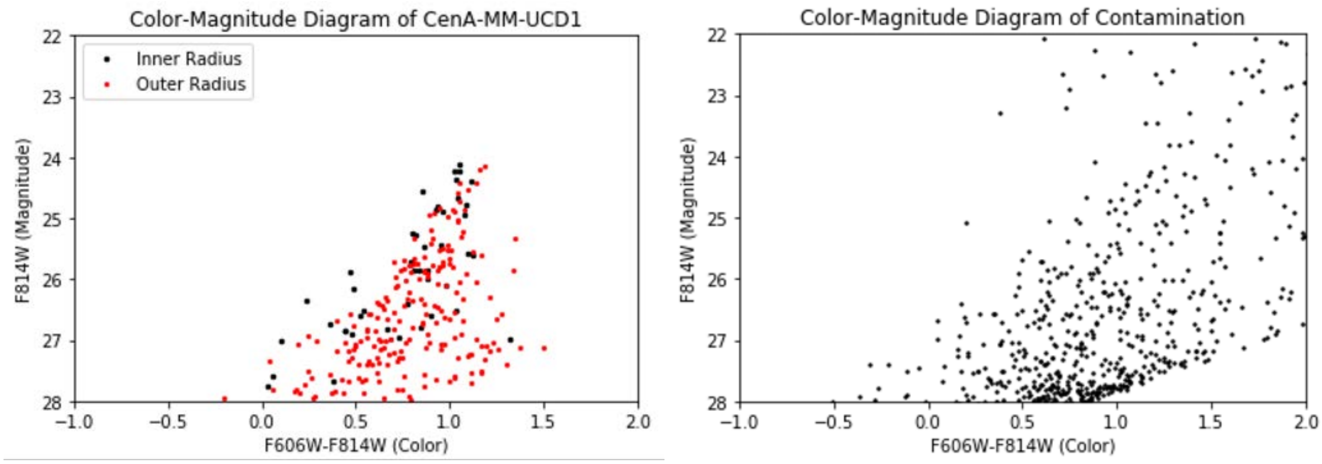

Fig. 5. Left panel: Color-magnitude diagram of the stars belonging to our target, which are mainly red-giant branch stars. The black points on the plot represent the stars within the inner radius of the galaxy (a distance of 65 pixels from the center of the galaxy). The red points represent the stars within the outer radius of the galaxy (a distance between 65 and 200 pixels from the center). Population of stars within the inner and outer radius fall within the same region of the CMD, which may conclude that there is no metallicity gradient present within CenA-MM-UCD1. There is no evidence of asymptotic giant branch (AGB) stars, which are more luminous with ages between 1-8 Gyrs. Right panel: Color-magnitude diagram of the stars located a distance of 300 pixels or more from the center of the galaxy. These stars represent the contamination, which consists of stars belonging to the Milky Way and background galaxies so distant that they appear as point sources within the HST images.

Color-Magnitude Diagram

After eliminating the "bad" stars from our data, we use the remaining data from our photometry, to create a CMD. This CMD allows us to analyze some properties of the stars within this galaxy. To create this CMD, we plot the magnitude of the stars from the F814W filter vs. the color or temperature of the stars. The color is found by taking the difference in magnitude in two different filters. We plot isochrones or stellar evolutionary models on our CMD to best fit our data (Dotter et al., 2008). These models depict how a star with a certain metallicity and age would evolve over time. From these models we are able to determine average metallicity or [Fe/H] value of the stars within our galaxy. Metallicity is a logarithmic quantity based on the relative abundance of iron with respect to hydrogen in the Sun. A positive [Fe/H] value means a star is more metal-rich than the Sun and a negative value means a star is more metal-poor than the Sun. In Figure 4, the isochrones are the three lines in red. The left-most isochrone has a metallicity of -2.5, the center model is -1.0, and the right-most model is -0.7, but all three are fixed at an age of 10 Gyrs. The average metallicity value of the stars within our galaxy is about -1.4. On our CMD, we plotted error bars to show the uncertainty in magnitude and color that was found using the artificial star tests. Using our data from the photometry and our CMD, we are able to identify some important properties of our galaxy.

3 RESULTS

From our CMD, we are able to determine that the majority of stars within our galaxy are in the red-giant branch (RGB) phase of a star's evolution, and have estimated ages larger than about 10 Gyrs. We separated the stars within the RGB from the rest of the stars on our CMD. In the left-most CMD of Figure 5, the red points represent the stars within the outer radius of our galaxy, which are located between 65 and 200 pixels from the center. The black points represent the stars within the inner radius of our galaxy, which are located a distance of less than 65 pixels from the center of the galaxy. Since the black and red points are located in the same region of the CMD, we are able to determine that there is no significant metallicity gradient within our galaxy. If there was a change in metallicity from the inner to the outer radius of the galaxy, then the red and black points would be located in different regions of the CMD (see isochrones in Fig.4). The right-most CMD shows the contamination, obtained by plotting stars with distances greater than 300 pixels from the galaxy center. This contamination consists of stars belonging to the Milky Way and background galaxies so distant that they appear as point sources on our HST images. In both CMDs there are no signs of any asymptotic giant branch (AGB) stars. These are stars that are more luminous than RGB stars, with ages between 1-8 Gyrs.

After analyzing our CMD, we created a stellar density map, Figure 6. This is a map of the x and y positions of the stars along the red-giant branch. The lighter boxes represent a larger quantity of stars within that region. The units of the color bar on the right are stars 25×25 pixels^2. The stellar density map shows that there are 0 stars in the center even though there are many. This is because the stars at the center are so closely packed together that the photometry is unable to individually resolve these stars. We created the stellar density map to determine if there was any noticeable signs of disruption by the host galaxy, CenA. However, from our map, there were no obvious signs of asymmetry or elongation in our galaxy, indicating that it is likely not in a state of disruption.

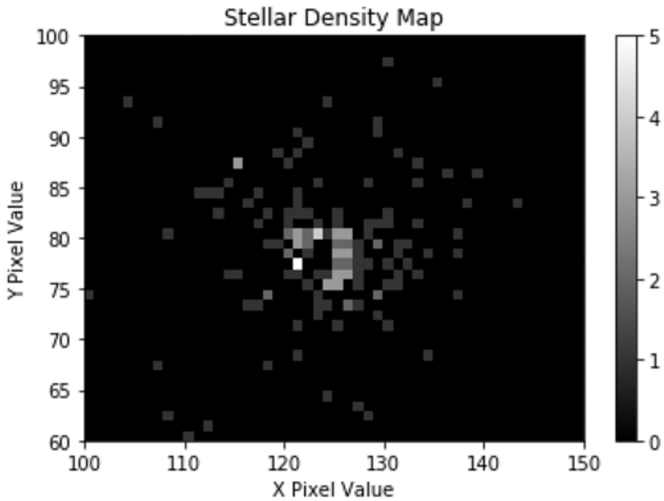

Fig. 6. Density map of the x and y spatial positions of the stars along the red-giant branch. The lighter boxes represent a larger quantity of stars within that region. The units of the color bar on the right are stars per 25 x 25 pixels^2. The stars within the center are unable to be resolved individually because they are too close together. This density map was derived to examine any sign of asymmetry or elongation due to a possible disruption from CenA. However, there is no clear evidence of this disruption within our density map.

4 DISCUSSION & CONCLUSIONS

Throughout this research, our goal was to determine if our target galaxy, CenA-MM-UCD1, is in a state of transition between a NSC and a UCD. We chose our galaxy because it is the first UCD with a resolved extended halo. We were trying to determine if this resolved extended halo was due to a disruption from CenA-MM-UCD1's host galaxy Centaurus A, which would help identify how UCDs are formed. In order to determine if our hypothesis was true, we look for properties characteristic of a NSC in our galaxy. The characteristics we investigated are younger population of stars, a gradient in metallicity, and signs of elongation or asymmetry. From our CMD, we determined that the stars within our galaxy were in the red-giant branch phase of stellar evolution. Stars within this phase are on the order of 10 or more Gyrs, which are older stars; younger stars would be stars that are less than 10 Gyrs, which we did not find on our CMD. However, younger stars could exist in the very center of our galaxy, but we might not be able to resolve them with our current technology. From our CMD of the RGB stars, we are able to determine that there is no evidence of a metallicity gradient within our galaxy since the stars within the inner radius and outer radius were located in the same region on the CMD. A metallicity gradient could exist, but better resolution is needed to detect it. The last characteristic we focused on is signs of disruption from the host galaxy, CenA. From our stellar density map, we determined that there are no obvious signs of disruption, which would appear as an elongation or asymmetry of our galaxy. Since the characteristics we were looking for were not shared by our galaxy, we have concluded that our galaxy does not appear to be in transition between a nuclear star cluster and a "normal UCD." In the future, we might obtain spectra to determine the stellar chemical composition of our galaxy and have a better understanding of the real nature of CenA-MM-UCD1.

ACKNOWLEDGEMENTS

The research presented here was partially supported by NASA grant HST-GO-15332.004-A.

REFERENCES

Crnojević, D., et al. 2016, ApJ, 823, 19
Dotter, A., et al. 2008, ApJS, 178, 89
Evstigneena et al. 2007, AJ, 133, 1722
Pfeffer et al. 2014, MNRAS, 444, 3670
Seth et al. 2010, ApJ, 714, 713
Seth et al. 2014, Nature, 513, 398